

Design and Motion Planning for a Zero-Reaction Manipulator

Evangelos Papadopoulos, Ahmed Abu-Abed

Department of Mechanical Engineering & Centre for Intelligent Machines
 McGill University
 Montreal, PQ, Canada H3A 2A7

ABSTRACT

In a number of industrial, space, or mobile systems applications, reaction forces and moments transmitted by a manipulator to its base are undesirable. Based on force and moment transmission analysis, a three DOF redundant manipulator design is selected aiming at reactionless motions. Dynamic reaction *forces* are eliminated by using force balancing. Reaction *moments* are eliminated by following reactionless paths, whose planning is simplified by rendering the dynamics of the system decoupled and invariant. The value of the synergy between design and planning is demonstrated by example cases. An additional advantage of this design is that the manipulator can be used either as a redundant system, or as a two DOF reactionless system.

I. INTRODUCTION

In many applications of advanced robotic systems, reaction forces transmitted by a manipulator to its base are highly undesirable. In an industrial setting, the accuracy of a rapidly accelerating manipulator will be degraded by vibrations induced by the transmission of large reaction forces to its mounts [1]. In space, dynamic forces due to the accelerating links of a manipulator will disturb the position and orientation of the satellite it may be mounted on [2,3]. If allowed to transmit reaction forces, manipulators operating in a micro-gravity environment will induce adverse effects on it [4]. Manipulators mounted on compliant mobile bases, be it a truck, a Mars rover, or the Shuttle Canadarm, will inevitably excite the base dynamics and result in poor dynamic performance and accuracy [5,6].

Moving a manipulator slowly is the simplest way to reduce the reactions to within acceptable levels. Reducing manipulator reactions by cost function minimization applied to redundant manipulators was proposed in [7]. Complete shaking force elimination can be achieved by fixing the center of gravity of the manipulator; this is accomplished by the addition of counterweights or by relocating the support point of the manipulator [1,8,9,10,11]. Minimization of the rocking moment can be accomplished by introducing counteracting torques. This is normally done using additional actuators with a preset inertia, along with a suitable controller [1]. However, these actuators cannot be used to enhance the system manipulative capabilities. In space, ma-

nipulator paths exist that will result in zero orientation disturbance for its free-floating (uncontrolled) spacecraft. However, following such paths will not eliminate reaction forces, i.e. the spacecraft will still translate. Use of such paths may also require relocating the spacecraft to some favorable initial position [5].

In this paper we analyze the problem of force and moment transmission by manipulators, and propose a number of guidelines that can result in reactionless motions. A three Degree-of-Freedom (DOF) nine link redundant manipulator design is selected with its three direct drive actuators base-mounted and sharing a common axis; with this configuration, reaction moments can be canceled if the actuators rotate in roughly opposite directions. The system Center of Mass (CM) is fixed by force balancing, and the dynamics of the system are decoupled and rendered invariant by adopting a parallel manipulator structure. This invariance feature simplifies the planning of reactionless paths, by requiring such paths to lie in fixed orientation joint space planes. With the restrictions on the trajectory, at least 3 DOF are required for a zero-reaction in-plane positioning task. The results show that motions planned in such a way result in minimal reactions, whereas non-reactionless motions are shown to transmit significant moments and forces. An advantage of this design is that the manipulator can be used either for tasks that require three DOF, or as a two DOF reactionless system.

II. FORCES AND MOMENTS

Consider a manipulator as an articulated mechanism to which its base applies a force \mathbf{f} and a moment \mathbf{n} , see Fig. 1.

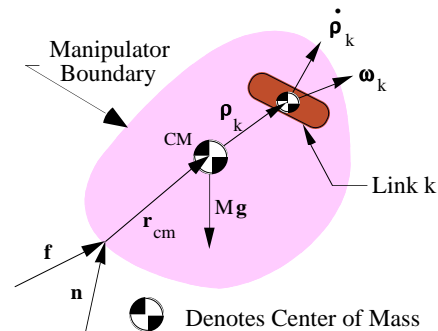


Fig.1. A manipulator boundary and applied forces & moments.

In the presence of gravity, the manipulator's weight is applied at its CM. If no other contact forces or moments are applied to the system, the following equation holds

$$\mathbf{f} + \mathbf{Mg} = \mathbf{f}_{\text{ext}} = \mathbf{M} \ddot{\mathbf{r}}_{\text{cm}} \quad (1)$$

where M is the total manipulator mass, \mathbf{g} is the acceleration of gravity, and $\ddot{\mathbf{r}}_{\text{cm}}$ is the acceleration of the system CM. Therefore, the force at the base is given by

$$\mathbf{f} = \mathbf{M} \ddot{\mathbf{r}}_{\text{cm}} - \mathbf{Mg} \quad (2)$$

and has a dynamic component, $\mathbf{M} \ddot{\mathbf{r}}_{\text{cm}}$, and a static component, $-\mathbf{Mg}$. Note that the latter is zero in space. The concern here is to eliminate the dynamic components of base reactions, since these are responsible for vibration and disturbances.

The dynamic components in Eq. (2) are zero if the system CM does not accelerate

$$\ddot{\mathbf{r}}_{\text{cm}} = \mathbf{0} \quad (3)$$

Equation (3) can be integrated twice with respect to time. Assuming zero initial velocity $\dot{\mathbf{r}}_{\text{cm}}$, Eq. (3) is equivalent to $\mathbf{r}_{\text{cm}} = \text{constant}$, in other words, for zero dynamic forces, the manipulator's CM has to be fixed with respect to the base frame. In principle, this condition can be achieved by design. The options include manipulator force balancing, or the use of additional base masses moving so as to cancel manipulator reaction forces. Although the second option is in principle feasible, the first one is more attractive due to its simplicity and will be employed here. Note that if the first joint is prismatic, a constant (or zero) reaction force would require either a non-actuated joint, or multiple manipulator actuators at the base moving in opposite directions. Both requirements are difficult to implement from a design point of view. On the other hand, if the first joint is rotary, dynamic reaction forces can be eliminated by the addition of counterweights.

The case of base moments is more complicated. Since the gravity force has no moment with respect to the system CM, the base moment, \mathbf{n} , is given by

$$\mathbf{n} = \mathbf{r}_{\text{cm}} \times \mathbf{f} + \frac{d}{dt} \left\{ \sum_{k=1}^L (\mathbf{I}_k \cdot \boldsymbol{\omega}_k + m_k \boldsymbol{\rho}_k \times \dot{\boldsymbol{\rho}}_k) \right\} \quad (4)$$

where L is the number of links, \mathbf{I}_k is the k^{th} link inertia, $\boldsymbol{\omega}_k$ its inertial angular velocity, m_k its mass, and $\boldsymbol{\rho}_k$ the vector from the system CM to the link CM, see Fig. 1. It can be recognized that the sum in Eq. (4) represents the angular momentum of the manipulator with respect to its CM [3]. Assuming that \mathbf{r}_{cm} is set equal to zero by design, then, for the base moment to cancel, Eq. (4) requires that this angular momentum is also zero, i.e. that

$$\sum_{k=0}^N \{ \mathbf{I}_k \cdot \boldsymbol{\omega}_k + m_k \boldsymbol{\rho}_k \times \dot{\boldsymbol{\rho}}_k \} = \mathbf{0} \quad (5)$$

where it was assumed that the initial angular momentum is zero. In general, unlike the linear momentum, the angular momentum cannot be integrated analytically to yield geometric conditions for $\mathbf{n} = \mathbf{0}$. Special trajectories that satisfy Eq. (4) could be found, but with great computational burden. However as shown in this paper, finding such trajectories can be simplified by proper manipulator design. Note that zero base reaction moments can be achieved by using additional base actuators like reaction wheels. This method is employed in space [2,3], and was used in the design of a high-acceleration minipositioner [1]. However, these additional actuators cannot be used to increase the DOFs of the manipulator. If no wheels are used and the first joint is revolute, $\mathbf{n} = \mathbf{0}$ would require that either the first joint is not actuated, or that multiple actuators are located at the base and move in such way that $\mathbf{n} = \mathbf{0}$. The latter method is employed here. A design based on the former method is currently under study.

From the above analysis, the following design guidelines emerge

- Force balance the manipulator to avoid dynamic base forces.
- To allow for the possibility of canceling base moments in some given direction, mount manipulator actuators at the base so that their common axis is in this direction.
- Use special planning techniques to maintain zero angular momentum. Since this step introduces an additional constraint, a task-redundant manipulator design should be used.

These guidelines are implemented on a 3 DOF parallel redundant planar manipulator having all revolute joints and with its three actuators mounted at the base and acting along the same axis. To maintain planar operation, the manipulator is assumed to be symmetric with respect to its plane of action.

III. MANIPULATOR DESIGN

This section focuses on the design of the 3 DOF parallel manipulator with nine mobile links shown in Fig. 2. This manipulator is redundant in terms of in-plane positioning, and was proposed as a finger for a mechanical hand [12]. As shown below, a certain combination of the manipulator's physical parameters, along with proper motion planning, results in zero-reactions transmitted to the base during motion.

As depicted in Fig. 2, the manipulator is composed of three parallel mechanisms; links 1-4-6 are always mutually parallel, and so are 2-5-8 and 3-7-9. Each set of parallel links can be made to rotate while the other links are either stationary or translating. The driving links, (1, 2, & 3), and their direct drive actuators are on the base; this characteristic

simplifies the decoupling of the manipulator's mass matrix and results in simpler dynamic equations [13]. As evident from Fig. 2, the following sets of links share common lengths: $l_1 = l_4 = l_6$, $l_5 = l_8$, and $l_3 = l_7$.

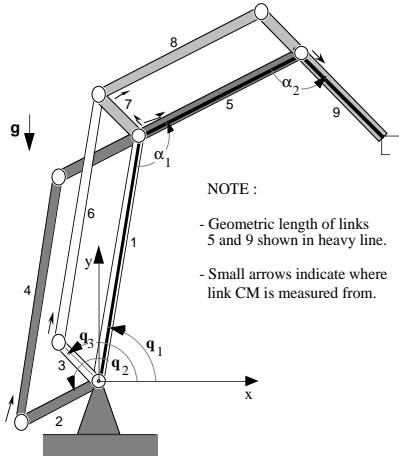


Fig.2. A 3 DOF 9-link parallel manipulator.

The dynamic equations for this manipulator are

$$\boldsymbol{\tau} = \mathbf{H}(\mathbf{q})\ddot{\mathbf{q}} + \mathbf{V}(\mathbf{q},\dot{\mathbf{q}}) + \mathbf{G}(\mathbf{q}) \quad (6)$$

where $\mathbf{q} = [q_1, q_2, q_3]^T$ is the vector of generalized coordinates (link absolute angles), $\boldsymbol{\tau} = [\tau_1, \tau_2, \tau_3]^T$ the vector of actuator torques, $\mathbf{H}(\mathbf{q})$ is the 3×3 manipulator mass matrix, $\mathbf{V}(\mathbf{q},\dot{\mathbf{q}}) = [v_1, v_2, v_3]^T$ is the vector of centripetal forces, and $\mathbf{G}(\mathbf{q}) = [g_1, g_2, g_3]^T$ is the gravity vector. Detailed expressions for \mathbf{V} and \mathbf{G} are given in Appendix A.

Since all three joint actuators share the same axis, the total moment applied to the base is given by

$$\mathbf{n}_B = -\mathbf{n} = -(\tau_1 + \tau_2 + \tau_3)\mathbf{k} \quad (7)$$

where \mathbf{k} is the unit z-axis vector. When the manipulator is not moving, then Eqs. (4) and (7) result in

$$\mathbf{n} = \mathbf{r}_{cm} \times \mathbf{f} = \mathbf{r}_{cm} \times \mathbf{M}\mathbf{g} = (g_1 + g_2 + g_3)\mathbf{k} \quad (8)$$

Eq. (8) shows that static balancing of the manipulator, (by setting all $g_i = 0$), results in $\mathbf{r}_{cm} = \mathbf{0}$. As discussed in Section II, a zero \mathbf{r}_{cm} has the effect of eliminating the base dynamic forces. Setting the g_i equal to zero yields three algebraic equations in terms of the geometric properties of the links, and the configuration \mathbf{q} , see Eq. (A3).

When the manipulator is moving, setting $\mathbf{n} = \mathbf{0}$ in Eq. (4) results in a complex equation relating accelerations, velocities and generalized coordinates. If $\mathbf{r}_{cm} = \mathbf{0}$, then Eq. (5) results in a constraint equation among velocities. In general, this equation cannot be integrated analytically to yield a relationship between the generalized coordinates, \mathbf{q} , useful for planning reaction-free trajectories. However, if \mathbf{H} is made invariant, then \mathbf{V} in Eq. (6) is zero, and Eq. (7) can be integrated twice as long as $\mathbf{r}_{cm} = \mathbf{0}$. Since the diagonal terms of \mathbf{H} are constant, see Eq. (A1), it suffices to set the

non-diagonal terms of \mathbf{H} , namely h_{12} , h_{13} , and h_{23} , equal to zero. Three additional algebraic equations are obtained and must be satisfied simultaneously with the ones for the g_i 's. Then, the dynamic equations given by Eq. (6) become

$$\begin{bmatrix} \tau_1 \\ \tau_2 \\ \tau_3 \end{bmatrix} = \begin{bmatrix} h_{11} & 0 & 0 \\ 0 & h_{22} & 0 \\ 0 & 0 & h_{33} \end{bmatrix} \begin{bmatrix} \ddot{q}_1 \\ \ddot{q}_2 \\ \ddot{q}_3 \end{bmatrix} \quad (9)$$

Next, the locations of the CMs of the nine links are chosen as the unknown design parameters. The six design constraint equations for $g_1, g_2, g_3, h_{12}, h_{13}$ and h_{23} , are written as

$$\begin{bmatrix} m_1 & 0 & 0 & m_4 & 0 & m_6 & 0 & 0 & 0 \\ 0 & m_2 & 0 & 0 & -m_5 & 0 & 0 & -m_8 & 0 \\ 0 & 0 & m_3 & 0 & 0 & 0 & m_7 & 0 & -m_9 \\ 0 & 0 & 0 & m_4 \frac{l_2}{l_1} & -m_5 & 0 & 0 & -m_8 & 0 \\ 0 & 0 & 0 & 0 & 0 & m_6 \frac{l_3}{l_1} & m_7 & 0 & -m_9 \\ 0 & 0 & 0 & 0 & 0 & 0 & 0 & -m_8 \frac{l_3}{l_5} & m_9 \end{bmatrix} \begin{bmatrix} l_{c1} \\ l_{c2} \\ l_{c3} \\ l_{c4} \\ l_{c5} \\ l_{c6} \\ l_{c7} \\ l_{c8} \\ l_{c9} \end{bmatrix} = \begin{bmatrix} -(m_5 + m_7 + m_8 + m_9)l_1 \\ m_9l_5 - m_4l_2 \\ -(m_8 + m_6)l_3 \\ m_9l_5 \\ -m_8l_3 \\ 0 \end{bmatrix} \quad (10)$$

where m_i ($i=1, \dots, 9$) are link masses, l_i ($i=1, \dots, 9$) are link lengths, and l_{ci} ($i=1, \dots, 9$) are distances of link CMs from points shown in Fig. 2. Using a weighted minimum norm method, this system of equations is solved, and the final manipulator geometric parameters are displayed in Table I.

Table I. Manipulator Parameters

i	l_i (m)	m_i (kg)	I_i (kgm ²)	l_{ci} (m)
1	0.50	7.00	0.2501	-0.2214
2	0.18	1.45	0.0025	-0.1111
3	0.20	2.00	0.0180	-0.1605
4	0.50	1.50	0.0199	0.2016
5	0.46	0.70	0.0215	-0.0110
6	0.50	1.50	0.0419	-0.0349
7	0.20	1.15	0.0143	-0.0682
8	0.46	0.50	0.0162	0.0032
9	0.30	0.25	0.0058	0.0027

IV. REACTIONLESS TRAJECTORY PLANNING

According to Eqs. (7) and (9), the base reaction moment is

$$\mathbf{n}_B = - (h_{11} \ddot{q}_1 + h_{22} \ddot{q}_2 + h_{33} \ddot{q}_3) \mathbf{k} \quad (11)$$

If the reaction moment is to be eliminated then the following equation must hold

$$\ddot{q}_1 + \lambda_2 \ddot{q}_2 + \lambda_3 \ddot{q}_3 = 0 \quad (12)$$

where $\lambda_2 = h_{22}/h_{11}$ and $\lambda_3 = h_{33}/h_{11}$ are constants. Eq. (12) is integrated to yield a constraint in terms of the link angles \mathbf{q} . With zero initial conditions for the rates, the integration results in

$$\dot{q}_1 + \lambda_2 \dot{q}_2 + \lambda_3 \dot{q}_3 = 0 \quad (13)$$

which is a manifestation of the zero angular momentum, see Eq. (5). Physically, this equation suggests that reactionless motion requires at least one joint to move opposite some other one. Since λ_2 and λ_3 are constants, the equation can be integrated again to yield

$$q_1 + \lambda_2 q_2 + \lambda_3 q_3 = b \quad (14)$$

where the constant b is called here the *pose constant*, because it depends on the initial set of link angles. Equation (14) represents a *plane* in the space of q_1 - q_2 - q_3 , with $\boldsymbol{\lambda} = [1, \lambda_2, \lambda_3]^T$ its normal vector. Moving in a reactionless path requires Eq. (14) to be satisfied. Furthermore, for a given initial configuration \mathbf{q} , the pose constant is set, and all via points and the target must be on the same plane in the \mathbf{q} space. Since a redundant manipulator can reach points in its workspace in more than one pose, it follows from Eq. (14) that a single x-y coordinate can have a range of b constants associated with it. Each of these b constants defines a different plane, but since the normal vector $\boldsymbol{\lambda}$ is fixed for a given manipulator, all these planes are parallel.

Given a point in the x-y plane, the range of pose constants b which correspond to it can be found using inverse kinematic relationships similar to those in [12]. A plot of feasible q_1 angles versus the pose constant b for two (x, y) points, is depicted in Fig. 3. This figure can also be used to determine if two points can be joined by a reactionless path. To this end, it suffices to have some plot overlap, such as the one shown in Fig. 3. For example, point (0.50, 0.50) is reachable from (0.55, 0.90) if the initial angle q_1 is between 1.6 and 1.9 rad.

Path planning can be facilitated if the set of points that can be accessed by a reactionless path from some initial configuration is known. To find this *reactionless workspace*, it is assumed that the first joint can rotate freely, while the relative joint angles α_1 and α_2 , comply with some given joint limits. From Fig. 2, α_1 and α_2 , are given as

$$\alpha_1 = q_2 - q_1 \quad (15a)$$

$$\alpha_2 = q_3 - q_2 + \pi \quad (15b)$$

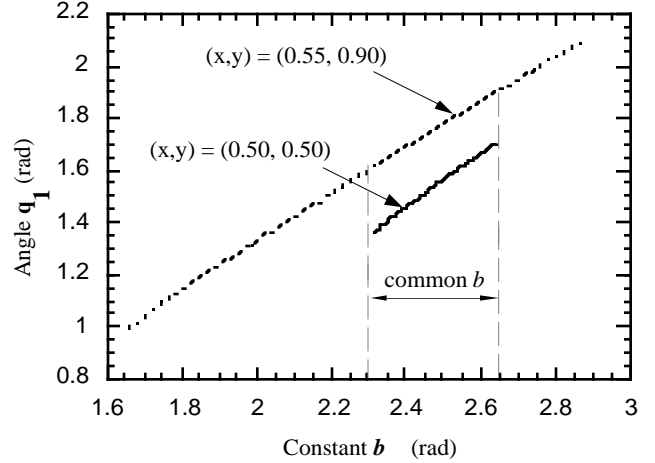


Fig.3. Range of q_1 and corresponding b pose constants for two (x, y) points

The forward kinematic equations for this manipulator are, see Fig. 2

$$x = l_1 \cos(q_1) - l_5 \cos(q_2) - l_9 \cos(q_3) \quad (16a)$$

$$y = l_1 \sin(q_1) - l_5 \sin(q_2) - l_9 \sin(q_3) \quad (16b)$$

Substituting Eq. (15) in Eqs. (16), and writing the result in matrix form, results in

$$\begin{bmatrix} x \\ y \end{bmatrix} = \begin{bmatrix} \cos(q_1) & -\sin(q_1) \\ \sin(q_1) & \cos(q_1) \end{bmatrix} \begin{bmatrix} l_1 - l_5 \cos(\alpha_1) + l_9 \cos(\alpha_1 + \alpha_2) \\ -l_5 \sin(\alpha_1) + l_9 \sin(\alpha_1 + \alpha_2) \end{bmatrix} \quad (17)$$

Furthermore, using Eqs. (14) and (15), q_1 itself can be expressed as

$$q_1 = \frac{b}{1 + \lambda_2 + \lambda_3} + \frac{\lambda_3(\pi - \alpha_2) - \alpha_1(\lambda_2 + \lambda_3)}{1 + \lambda_2 + \lambda_3} = b^* + \phi(\alpha_1, \alpha_2) \quad (18)$$

where $b^* = b/(1 + \lambda_2 + \lambda_3)$ is a constant, and ϕ an angle function of α_1 and α_2 . Substituting Eq. (18) in Eq. (17) yields

$$\begin{bmatrix} x \\ y \end{bmatrix} = \begin{bmatrix} c(b^*) & -s(b^*) \\ s(b^*) & c(b^*) \end{bmatrix} \begin{bmatrix} c(\phi) & -s(\phi) \\ s(\phi) & c(\phi) \end{bmatrix} \begin{bmatrix} l_1 - l_5 c(\alpha_1) + l_9 c(\alpha_1 + \alpha_2) \\ -l_5 s(\alpha_1) + l_9 s(\alpha_1 + \alpha_2) \end{bmatrix} \quad (19)$$

where $c()$, $s()$ denote the cosine and the sin of an angle. For a given initial pose, b and therefore b^* , are fixed. Hence, all the points that can be accessed starting from an initial pose can be found by varying the relative joint angles in the allowed range given by

$$lowlim_i \leq \alpha_i \leq uprlim_i \quad i = 1, 2 \quad (20)$$

Since the pose constant only appears in the first rotation matrix in Eq. (19), the *shape* of the reactionless workspace is independent of this constant. However, its *orientation* on the Cartesian plane depends on it. The reactionless workspace can be plotted in the Cartesian plane using Eq. (19) above, with α_i varying in the range given by Eq. (20). One such plot is shown in Fig. 4; any two points in this

workspace, shown as the dark gray region, can be connected by a reactionless path.

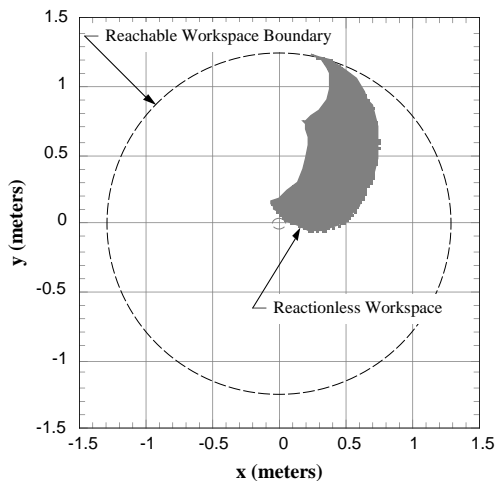


Fig.4. Reactionless workspace for $b = 2.4$ rad.

V. SIMULATION RESULTS & DISCUSSION

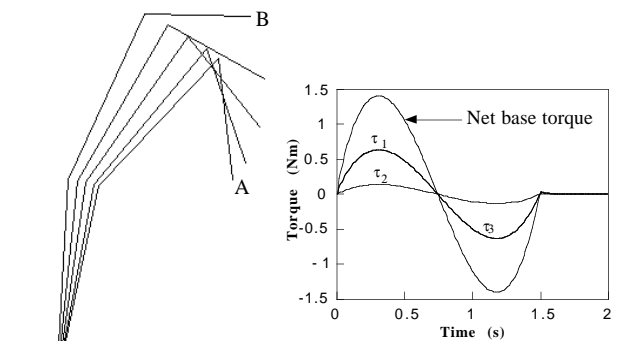
The dynamic equations of the 3 DOF parallel manipulator, shown in Appendix A, were programmed into MATLAB. The linear system of Eq. (10) was used to compute the physical parameters of the manipulator, required for reactionless motions. These parameters result in a manipulator which transmits zero dynamic forces at the base.

To calculate the reaction moments at the base, an initial and final point A and B were chosen from one reactionless region as follows: $(x_A, y_A) = (0.50, 0.50)$ and $(x_B, y_B) = (0.55, 0.90)$. The corresponding pose constant was $b = 2.4$ rad, and the travel time was set at 1.5 s. To test the effect of different paths on the total base reactions, the following three paths were chosen

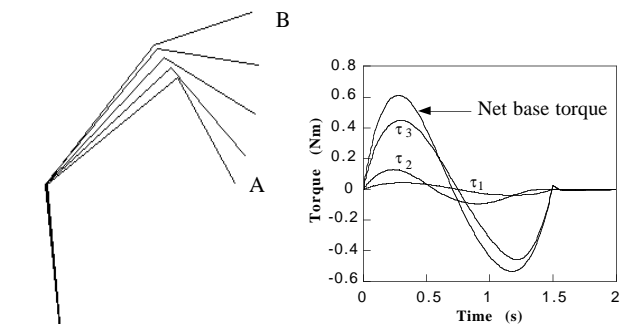
1. A path planned in Cartesian space, independent of any reactionless requirements.
2. A path planned in the configuration \mathbf{q} space; the path did not adhere to any reactionless plane.
3. A reactionless path. In Cartesian space, the path was identical to that in case 2 above. The x - y pairs along with the b constant determine the initial and final angles of the manipulator, \mathbf{q}_A and \mathbf{q}_B , see Eqs. (14) and (16). The path was a straight line in joint space connecting \mathbf{q}_A and \mathbf{q}_B , both lying on the plane defined by Eq. (14).

Quintic polynomial trajectories were used in the simulation in order to have continuous joint velocity and acceleration profiles. A computed torque control scheme was employed to determine the motor torques required, and the control gains were kept the same in all three cases. The required actuator torques τ_1 , τ_2 , and τ_3 , as well as the resultant base reaction are shown in Fig. 5. Snapshots of the corresponding motion sequences of links 1, 5 and 9 are also shown. As depicted in Figs. 5 (a) and (b), the resulting moment is

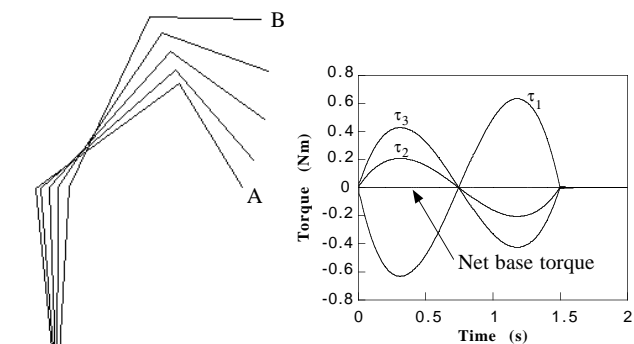
relatively high for cases 1 and 2 since no reactionless plane is adhered to. For case 3, Fig 5 (c) shows that throughout the reactionless trajectory the base moment is zero.



(a) Case 1



(b) Case 2



(c) Case 3

Fig.5. Manipulator snapshots and corresponding torque profiles. (a) Path planned in Cartesian space, (b) Path planned in joint space, (c) Reactionless path.

Although the above analysis indicates zero base reactions, small deviations from the ideal zero reaction case may occur in practice. Sources of such deviations include manufactur-

ing errors, neglected small unbalanced friction in the direct drive actuators, and manipulator unbalance due to a payload. However, in all these cases the proposed design will eliminate the most significant base reactions which are due to manipulator accelerating links.

Finally, note that in principle higher DOF spatial reactionless manipulators can be constructed using as building blocks two or three DOF reactionless manipulators. This combination is possible, since a manipulator which transmits zero dynamic forces and moments to its base is dynamically equivalent to a point mass. Serially connecting two reactionless planar manipulators, is equivalent to adding a point mass to the last link of the first manipulator, and this can be compensated for by designing appropriately the first manipulator. Since the second manipulator's base motor axes orientation can be arbitrary, choosing a suitable orientation can result in reactionless trajectories in three-dimensional space. However, the design of such manipulator would be far from trivial.

VI. CONCLUSIONS

Based on analysis of the force and moment transmission problem by manipulators, a three DOF redundant manipulator design was selected aiming at reactionless motions. The system center of mass was fixed by static balancing, and the dynamics of the system were decoupled and rendered invariant. The latter feature simplified the planning of reactionless paths, by requiring that such paths belong in fixed orientation planes in the joint space. Motions planned in such a way result in minimal reactions, whereas non-reactionless motions are shown to transmit significant reactions. An additional advantage of this design is that the manipulator can be used either as a redundant system, or as a two DOF reactionless system.

VII. ACKNOWLEDGMENTS

The support of this work by the Fonds pour la Formation de Chercheurs et l'Aide a la Recherche (FCAR), and by the Natural Sciences and Engineering Council of Canada (NSERC) is gratefully acknowledged.

REFERENCES

- [1] Karidis, J.P., et al, "The Hummingbird Mini-positioner - Providing Three Axis Motion at 50 G's With Low Reactions," *Proc. 1992 IEEE Conf. Robotics and Automation*, Nice, France, May 1992.
- [2] Dubowsky, S. and Torres, M.A., "Path Planning for Space Manipulators to Minimize Spacecraft Attitude Disturbance," *Proc. 1991 IEEE Conf. Robotics and Automation*, Sacramento, CA, April 1991.
- [3] Papadopoulos, E. and Dubowsky, S., "On the Nature of Control Algorithms for Free-floating Space Manipulators," *IEEE Trans. on Robotics and Autom.*, Vol. 7, No. 6, Dec. 1991, pp. 750-758.

- [4] Rohn, D., et al, "Microgravity Robotics Technology Program," *ISA/88 Int. Conf.*, Houston, TX, 1988.
- [5] Erb, B., "Canada's Mobile Servicing System," *Space Techn.*, Vol. 10, No 1/2, pp. 19-25, 1990.
- [6] West, H., et al. "Experimental Simulation of Manipulator Base Compliance," in *Experimental Robotics I*, V. Hayward and O. Khatib (Eds.), Lect. Notes in Control and Information Sciences #139, Springer Verlag, 1990.
- [7] Quinn, R.D., et al., "Redundant Manipulators for Momentum Compensation in a Micro-Gravity Environment," *AIAA Guidance, Navigation, and Control Conf.*, Minneapolis, MN, Aug. 1988.
- [8] Berkof, R.S., et al., "Balancing of Linkages," *Shock and Vibration Digest.*, 9, No. 6, pp. 3-10, 1977.
- [9] Walker, M.J. and Oldham, K., "General Theory of Force Balancing Using Counterweights," *Mech. & Machine Theory*, 13, pp. 175-185, 1978.
- [10] Kazerooni, H., "Design and Analysis of the Statically Balanced Direct-Drive Robot Manipulator," *Robotics and Computer Integrated Manufacturing*, 6, No. 4, pp. 287-293, 1989.
- [11] Kaufman, R.E. and Sandor, G.N., "Complete Force Balancing of Spatial Linkages," *ASME J. of Engineering for Industry*, 1971, pp. 620-626.
- [12] Youcef-Toumi, K. and Yahiaoui, M., "The Design of a Mini Direct-Drive Finger With Decoupled Dynamics," *ASME 1988 WAM*, pp. 411-415.
- [13] Asada, H. and Youcef-Toumi, K., *Direct-Drive Robots*, MIT Press, 1987.

APPENDIX A

For the 3 DOF manipulator in Fig. 2, the components of the mass matrix \mathbf{H} are

$$\begin{aligned}
 h_{11} &= I_1 + I_4 + I_6 + m_1 l_{c1}^2 + m_4 l_{c4}^2 + m_6 l_{c6}^2 + (m_5 + m_7 + m_8 + m_9) l_1^2 \\
 h_{12} &= (m_4 l_2 l_{c4} - m_5 l_1 l_{c5} - m_8 l_1 l_{c8} - m_9 l_1 l_5) \cos(q_1 - q_2) \\
 h_{13} &= (m_6 l_3 l_{c6} + m_7 l_1 l_{c7} + m_8 l_1 l_7 - m_9 l_1 l_{c9}) \cos(q_1 - q_3) \\
 h_{22} &= I_2 + I_5 + I_8 + m_2 l_{c2}^2 + m_5 l_{c5}^2 + m_8 l_{c8}^2 + m_4 l_2^2 + m_9 l_5^2 \\
 h_{23} &= (m_9 l_5 l_{c9} - m_8 l_7 l_{c8}) \cos(q_2 - q_3) \\
 h_{33} &= I_3 + I_7 + I_9 + m_3 l_{c3}^2 + m_7 l_{c7}^2 + m_9 l_{c9}^2 + m_6 l_3^2 + m_8 l_7^2 \quad (A1)
 \end{aligned}$$

The components of the \mathbf{V} and \mathbf{G} vectors in Eq. (6) are

$$\begin{aligned}
 v_1 &= (m_4 l_2 l_{c4} - m_5 l_1 l_{c5} - m_8 l_1 l_{c8} - m_9 l_1 l_5) \sin(q_1 - q_2) \dot{q}_2^2 \\
 &\quad + (m_6 l_3 l_{c6} + m_7 l_1 l_{c7} + m_8 l_1 l_7 - m_9 l_1 l_{c9}) \sin(q_1 - q_3) \dot{q}_3^2 \quad (A2) \\
 v_2 &= (-m_4 l_2 l_{c4} + m_5 l_1 l_{c5} + m_8 l_1 l_{c8} + m_9 l_1 l_5) \sin(q_1 - q_2) \dot{q}_1^2 \\
 &\quad - (m_8 l_7 l_{c8} + m_9 l_5 l_{c9}) \sin(q_2 - q_3) \dot{q}_3^2 \\
 v_3 &= (-m_6 l_3 l_{c6} - m_7 l_1 l_{c7} - m_8 l_1 l_7 + m_9 l_1 l_{c9}) \sin(q_1 - q_3) \dot{q}_1^2 \\
 &\quad + (m_8 l_7 l_{c8} - m_9 l_5 l_{c9}) \sin(q_2 - q_3) \dot{q}_2^2 \\
 g_1 &= (m_1 l_{c1} + m_4 l_{c4} + m_6 l_{c6} + (m_5 + m_7 + m_8 + m_9) l_1) g \cos(q_1) \\
 g_2 &= (m_2 l_{c2} + m_4 l_2 - m_5 l_{c5} - m_8 l_{c8} - m_9 l_5) g \cos(q_2) \\
 g_3 &= (m_3 l_{c3} + m_6 l_3 + m_7 l_{c7} + m_8 l_7 - m_9 l_{c9}) g \cos(q_3) \quad (A3)
 \end{aligned}$$